SUPPLEMENTARY MATERIALS

Molecular Structures of Fluid Phase Phosphatidylglycerol Bilayers as Determined by Small Angle Neutron and X-ray Scattering

Jianjun Pan,[a,] Frederick A. Heberle,[a] Stephanie Tristram-Nagle,[b] Michelle Szymanski,[c] Mary Koepfinger,[c] John Katsaras[a,d,e] and Norbert Kučerka[e,f]*

[a]Biology and Soft Matter Division, Neutron Sciences Directorate, Oak Ridge National Laboratory, Oak Ridge, TN, 37831-6100, USA

[b]Biological Physics Group, Department of Physics, Carnegie Mellon University, Pittsburgh, PA, 15213, USA

[c]Douglass Residential College, Rutgers University, New Brunswick, NJ, 08901, USA

[d]Joint Institute for Neutron Sciences, Oak Ridge National Laboratory, Oak Ridge, TN, 37831-6453, USA

[e]Canadian Neutron Beam Centre, National Research Council, Chalk River, Ontario, Canada K0J 1J0

[f]Department of Physical Chemistry of Drugs, Faculty of Pharmacy, Comenius University, Odbojárov 10, 832 32 Bratislava, Slovakia

Primary scattering data

Figure S1 shows the primary X-ray (panel A) and neutron (panel B) scattering data obtained from DOPG vesicles in H_2O and D_2O, respectively, after correcting for air and water scattering. The isotropic 2D scattering data is reduced to a 1D scattering curve (intensity vs. q) using standard radial averaging procedures, whereby detector pixels are binned into discrete q values. The *I versus q* data obtained in this manner are related to the vesicle form factor through Eq. 2 in the main text.

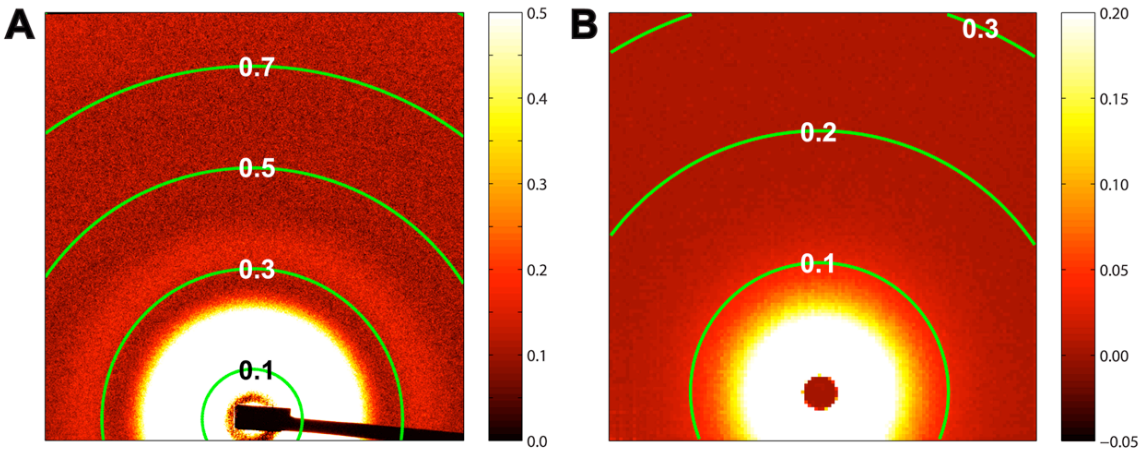

Fig. S1. Background subtracted 2D scattering data of DOPG vesicles at 30°C. (A) X-ray data of DOPG vesicles in H_2O. (B) Neutron data of DOPG vesicles in 100% D_2O. The scattering vector q range is indicated by the solid green contour lines (units of $Å^{-1}$). The relative scattering intensity is indicated by the corresponding color bars. The dark paddle-shaped region in (A) and the red circular-shaped region in (B) are beamstops (to block the primary beam) used in X-ray and neutron scattering experiments, respectively.

SDP model analysis

Bilayer structural parameters are determined through the simultaneous analysis of neutron and X-ray small angle scattering data using the scattering density profile (SDP) model developed for PG lipids [S1]. Guided by MD simulations, the PG lipid was "parsed" into component groups chosen on the basis that each group has the same functional form (e.g., Gaussian) for all the different contrast conditions (i.e., X-ray and neutron scattering density data, Figs. 2C and 2D, respectively). Three Gaussians are used to describe the lipid headgroup, one each for the carbonyl-glycerol (CG), phosphate (PG1) and terminal glycerol (PG2) moieties. The total hydrocarbon region (i.e., the sum of the CH_2, CH and CH_3 groups) is represented by an error function. The CH and CH_3 groups

are each described by a single Gaussian, which are then subtracted from the error function to obtain the CH_2 distribution. The distribution of the water component is defined by complementarity with the other lipid components by requiring that all volume probabilities sum to unity at each point along *z* (Fig. 2E). In this way, the model captures all of the features of the different SDPs, while satisfying the spatial conservation principle [S2]. Finally, the analytical X-ray and neutron form factors, which are used to fit to experimental scattering data, were obtained by the Fourier transform of the electron and the various neutron scattering length densities, which were based on the SDP model.

The following tables contain the complete list of bilayer structural parameters obtained from a global nonlinear least-square analysis of the neutron and X-ray data. Double asterisks (**) denote fixed values (i.e., values which are not varied in the fit), and single asterisks (*) denote "soft" constrained parameters with target values given in parentheses (see section 2.4 of the main text).

Figures show the X-ray (panel A) and the neutron form factors (panel B) obtained at three different contrast conditions. These form factors are available for a direct comparison to simulated data (as outlined in [S3]) in addition to being used in SDP model-based analysis. We employ the latter method in this study. The model form factor derived from the best-fit values is shown in panels A and B by the solid lines. The component volume probabilities corresponding to the best-fit parameters are shown in panel E. Electron density and neutron scattering length densities are calculated from the volume probabilities, and are shown in panels C and D, respectively. The vertical dashed-dotted lines indicate half of the phosphate-phosphate distance ($D_{HH}/2$) and overall bilayer thickness ($D_B/2$). The hydrocarbon thickness $2D_C$ is depicted by the horizontal dashed-dotted lines.

Table S1 Length (Å), area (Å^2), and volume (Å^3) parameters for DLPG bilayers (estimated uncertainty of ±2%).

Figure	S1	S2	S3	S4
T	20°C	30°C	50°C	60°C
V_L	945.9**	953.6**	962.4**	971.5**
V_{HL}	291.0**	291.0**	291.0**	291.0**
R_{CG}	0.51*(0.52)	0.51*(0.52)	0.51*(0.52)	0.52*(0.52)
R_{PG1}	0.16*(0.16)	0.16*(0.16)	0.16*(0.16)	0.16*(0.16)
r	1.79*(1.86)	1.83*(1.86)	1.85*(1.86)	1.83*(1.86)
r_{12}	0.71*(0.71)	0.71*(0.71)	0.71*(0.71)	0.71*(0.71)
D_B	29.9	29.1	27.8	27.2
D_{HH}	30.6	30.6	30.0	29.6
2Dc	20.7	20.2	19.4	19.0
D_{H1}	5.0	5.2	5.3	5.3
A	63.4	65.6	69.2	71.6
z_{CG}	11.1	10.7	10.2	10.0
σ_{CG}	2.21	2.15	2.11	2.05
z_{PG1}	15.8	15.6	15.2	15.1
σ_{PG1}	2.94	2.76	2.71	2.98
z_{PG2}	16.1	16.1	15.8	15.6
σ_{PG2}	3.30**	3.30**	3.30**	3.30**
z_{CH}	NA	NA	NA	NA
σ_{CH}	NA	NA	NA	NA
σ_{HC}	2.55*(2.44)	2.52*(2.44)	2.49*(2.44)	2.48*(2.44)
σ_{CH3}	4.10	3.77	3.75	3.76

**fixed parameters.

*soft-constrained parameters with target values shown in parentheses.

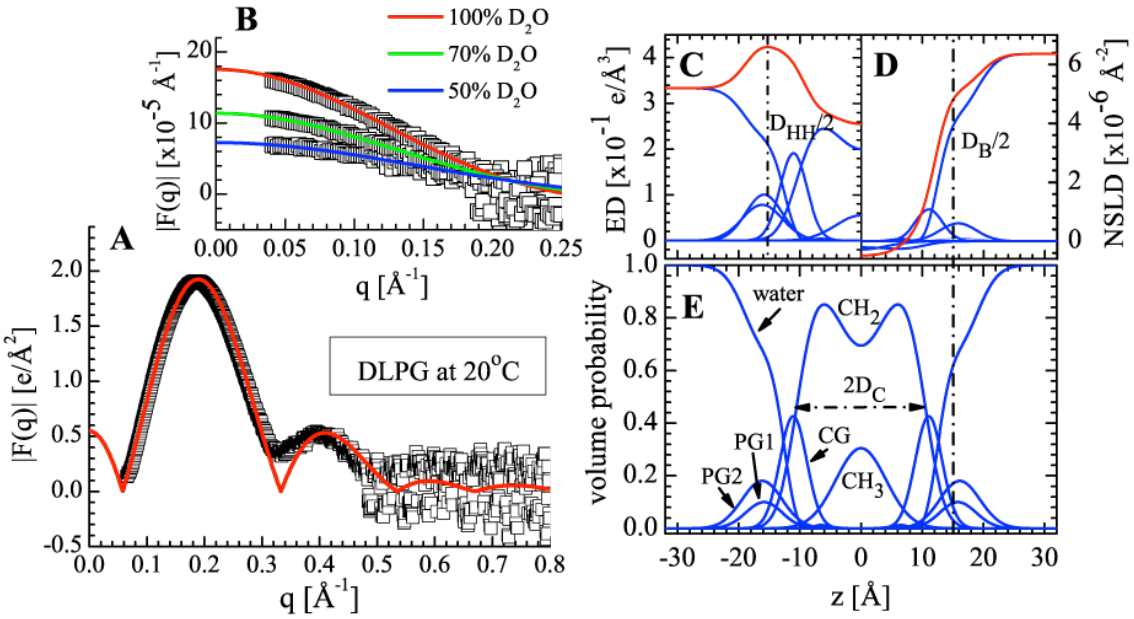

Fig. S2. SDP model analysis of DLPG at 20°C.

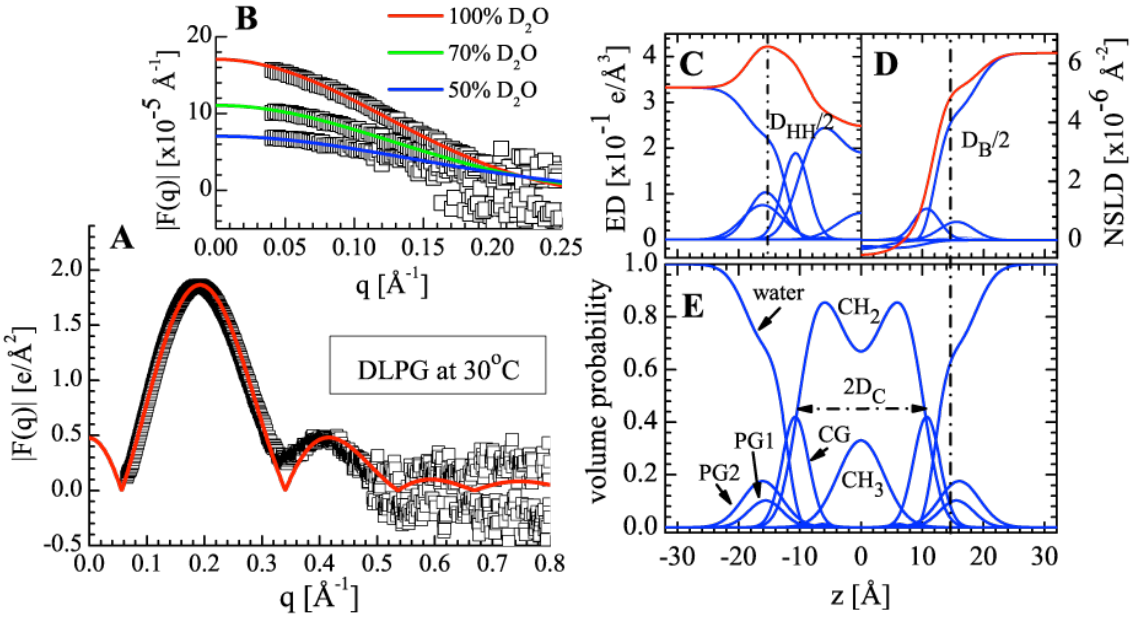

Fig. S3. SDP model analysis of DLPG at 30°C.

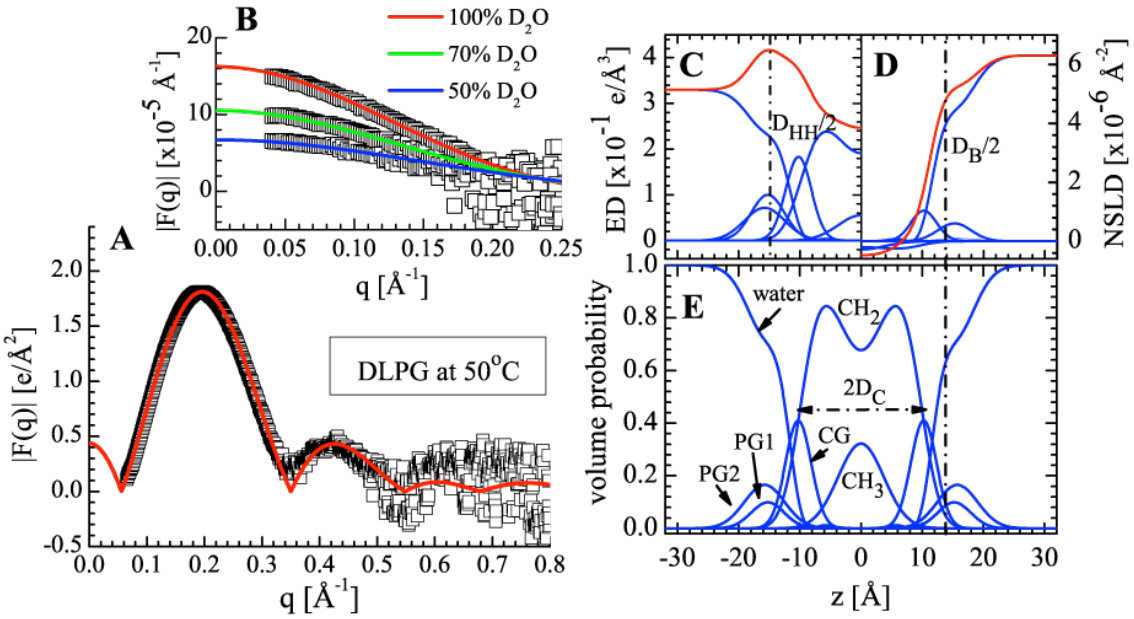

Fig. S4. SDP model analysis of DLPG at 50°C.

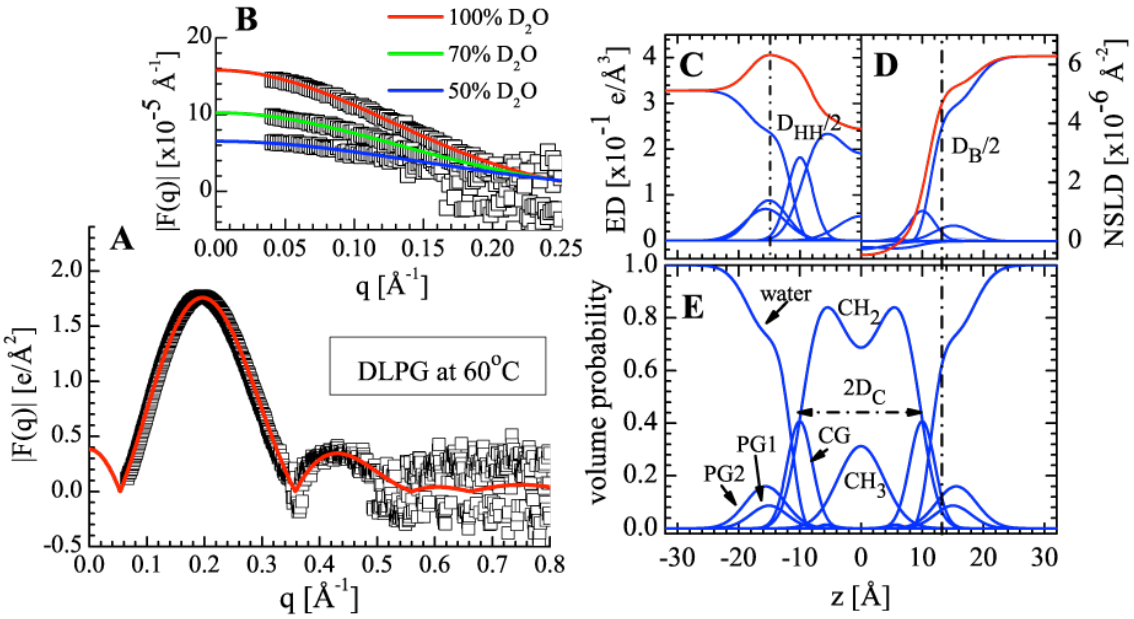

Fig. S5. SDP model analysis of DLPG at 60°C.

Table S2 Length (Å), area (Å^2), and volume (Å^3) parameters for DMPG, DPPG, and DSPG bilayers (estimated uncertainty of ±2%).

Figure	S5	S6	S7	S8	S9	S10
Lipid	DMPG	DMPG	DMPG	DPPG	DPPG	DSPG
T	30^{o}C	50^{o}C	60^{o}C	50^{o}C	60^{o}C	60^{o}C
V_L	1057.4**	1074.0**	1080.9**	1188.8**	1198.1**	1305.0**
V_{HL}	291.0**	291.0**	291.0**	291.0**	291.0**	291.0**
R_{CG}	0.51*(0.52)	0.49*(0.52)	0.49*(0.52)	0.50*(0.52)	0.51*(0.52)	0.51*(0.52)
R_{PG1}	0.16*(0.16)	0.16*(0.16)	0.16*(0.16)	0.16*(0.16)	0.16*(0.16)	0.16*(0.16)
r	1.76*(1.86)	1.95*(1.86)	1.94*(1.86)	1.87*(1.86)	1.90*(1.86)	1.87*(1.86)
r_{12}	0.71*(0.71)	0.71*(0.71)	0.71*(0.71)	0.71*(0.71)	0.71*(0.71)	0.71*(0.71)
D_B	32.5	31.4	30.9	35.5	34.5	38.2
D_{HH}	35.4	34.6	34.0	38.8	37.6	40.8
2Dc	23.6	22.9	22.6	26.8	26.1	29.7
D_{H1}	5.9	5.8	5.7	6.0	5.7	5.5
A	65.1	68.4	69.9	67.0	69.4	68.3
z_{CG}	12.7	12.0	11.7	14.4	13.9	15.9
σ_{CG}	2.26	2.52	2.41	2.58	2.32	2.48
z_{PG1}	17.9	17.6	17.2	19.6	19.1	21.0
σ_{PG1}	2.46	2.38	2.55	2.17	2.87	2.76
z_{PG2}	18.4	18.0	17.7	19.8	19.5	20.4
σ_{PG2}	3.30**	3.30**	3.30**	3.30**	3.30**	3.30**
z_{CH}	NA	NA	NA	NA	NA	NA
σ_{CH}	NA	NA	NA	NA	NA	NA
σ_{HC}	2.46*(2.44)	2.64*(2.44)	2.62*(2.44)	2.54*(2.44)	2.50*(2.44)	2.43*(2.44)
σ_{CH3}	3.71	3.50	3.52	2.97	3.14	2.80

**fixed parameters.

*soft-constrained parameters with target values shown in parentheses.

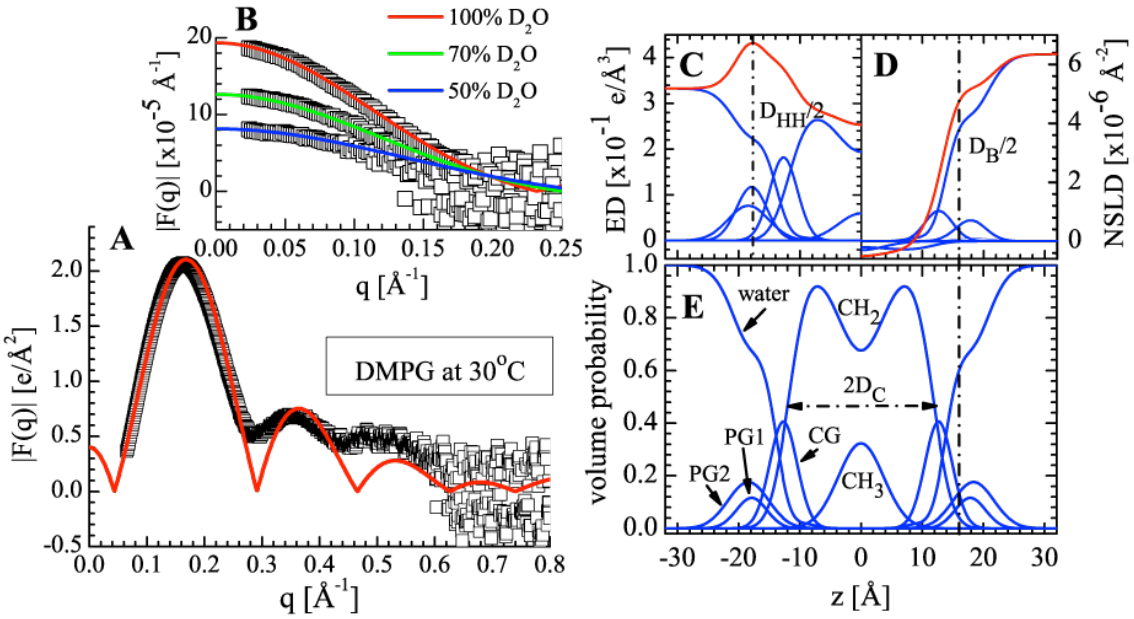

Fig. S6. SDP model analysis of DMPG at 30°C. As discussed in the main text, the two non-zero minima in the data imply an asymmetric bilayer distribution.

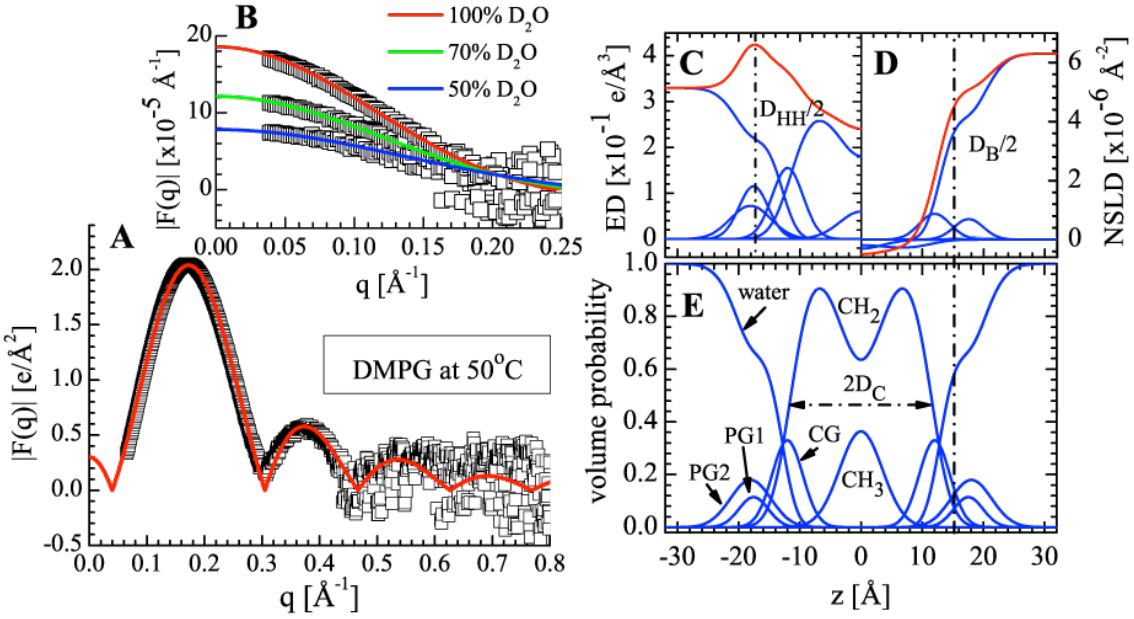

Fig. S7. SDP model analysis of DMPG at 50°C.

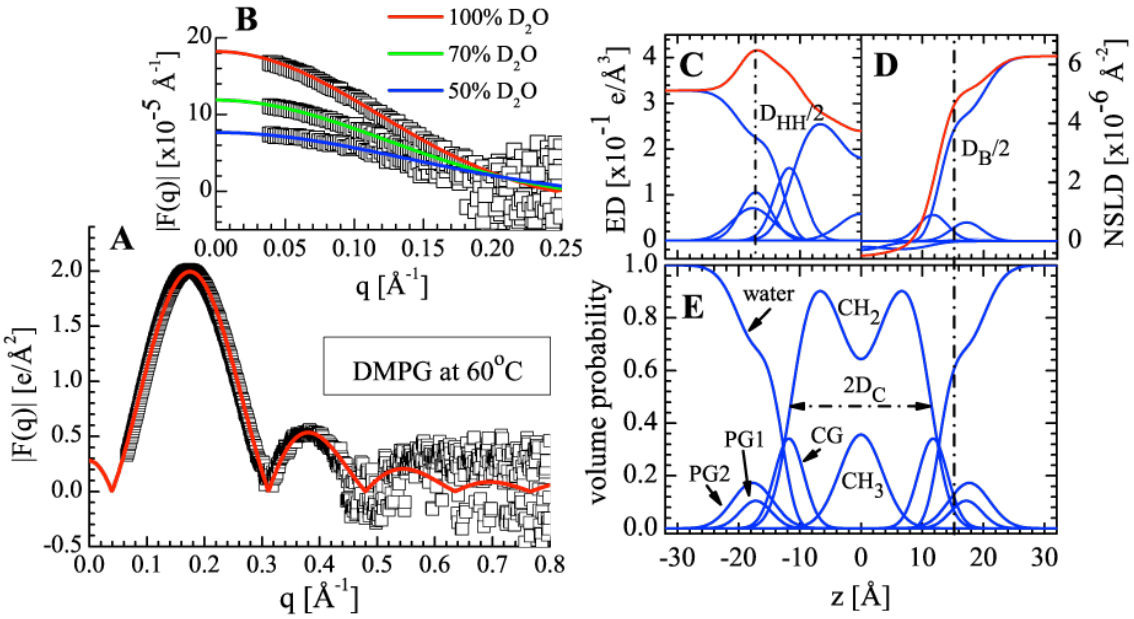

Fig. S8. SDP model analysis of DMPG at 60°C.

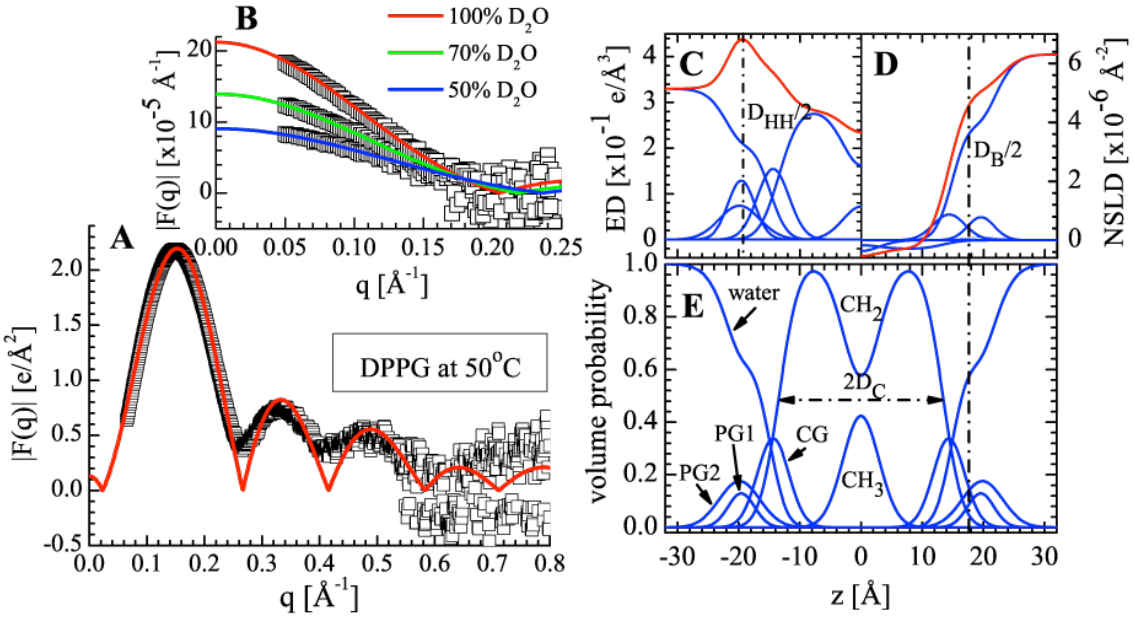

Fig. S9. SDP model analysis of DPPG at 50°C.

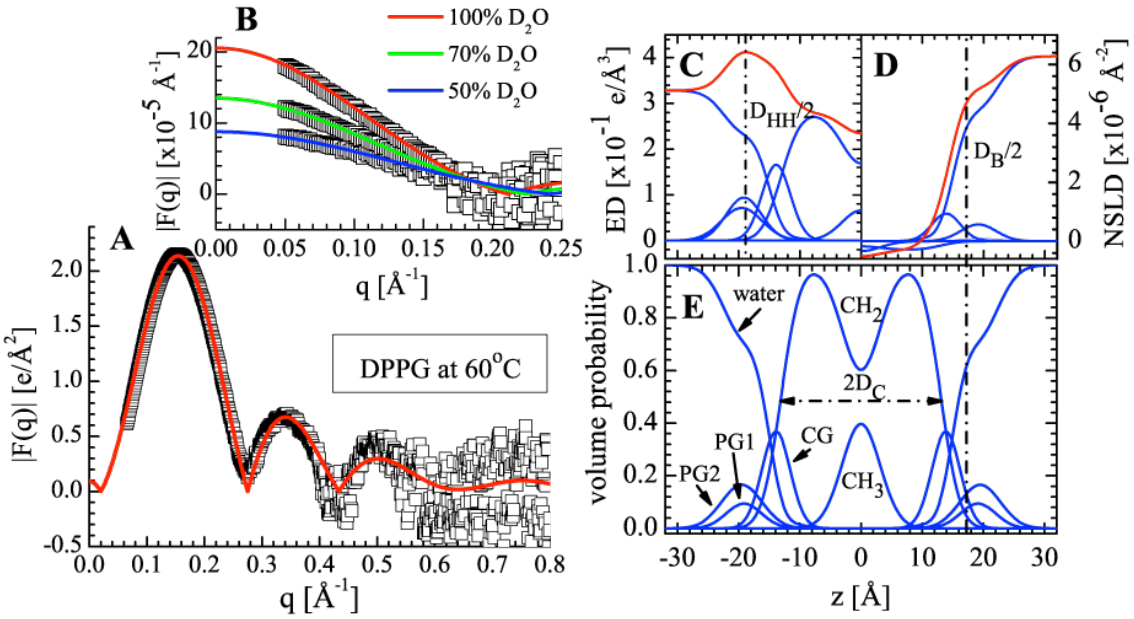

Fig. S10. SDP model analysis of DPPG at 60°C.

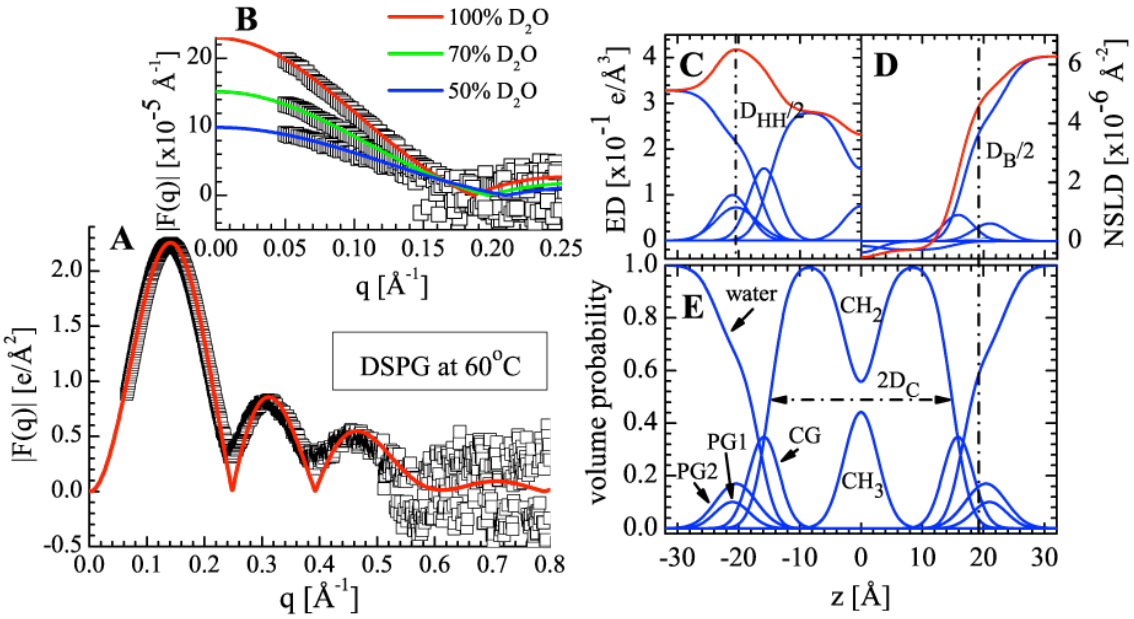

Fig. S11. SDP model analysis of DSPG at 60°C.

Table S3 Length (Å), area (Å^2), and volume (Å^3) parameters for POPG bilayers (estimated uncertainty of ±2%).

Figure	S11	S12	S13	S14
Lipid	POPG	POPG	POPG	POPG
T	20^{o}C	30^{o}C	50^{o}C	60^{o}C
V_L	1201.9**	1208.7**	1233.7**	1243.6**
V_{HL}	291.0**	291.0**	291.0**	291.0**
R_{CG}	0.51*(0.52)	0.52*(0.52)	0.51*(0.52)	0.52*(0.52)
R_{PG1}	0.16*(0.16)	0.16*(0.16)	0.16*(0.16)	0.16*(0.16)
r	1.79*(1.86)	1.85*(1.86)	1.91*(1.86)	1.92*(1.86)
r_{12}	0.70*(0.71)	0.70*(0.71)	0.70*(0.71)	0.70*(0.71)
D_B	37.3	36.6	35.5	34.9
D_{HH}	37.8	37.4	36.4	36.2
2Dc	28.3	27.8	27.1	26.7
D_{H1}	4.8	4.8	4.6	4.7
A	64.4	66.1	69.5	71.3
z_{CG}	14.7	14.5	14.1	13.8
σ_{CG}	2.39	2.28	2.19	2.22
z_{PG1}	19.2	19.0	18.5	18.3
σ_{PG1}	2.50	2.54	2.77	2.75
z_{PG2}	20.9	20.7	20.2	20.0
σ_{PG2}	3.30**	3.30**	3.30**	3.30**
z_{CH}	7.8**	7.8**	7.8**	7.8**
σ_{CH}	3.20**	3.20**	3.20**	3.20**
σ_{HC}	2.63*(2.44)	2.56*(2.44)	2.54*(2.44)	2.54*(2.44)
σ_{CH3}	3.58	3.51	3.38	3.26

**fixed parameters.

*soft-constrained parameters with target values shown in parentheses.

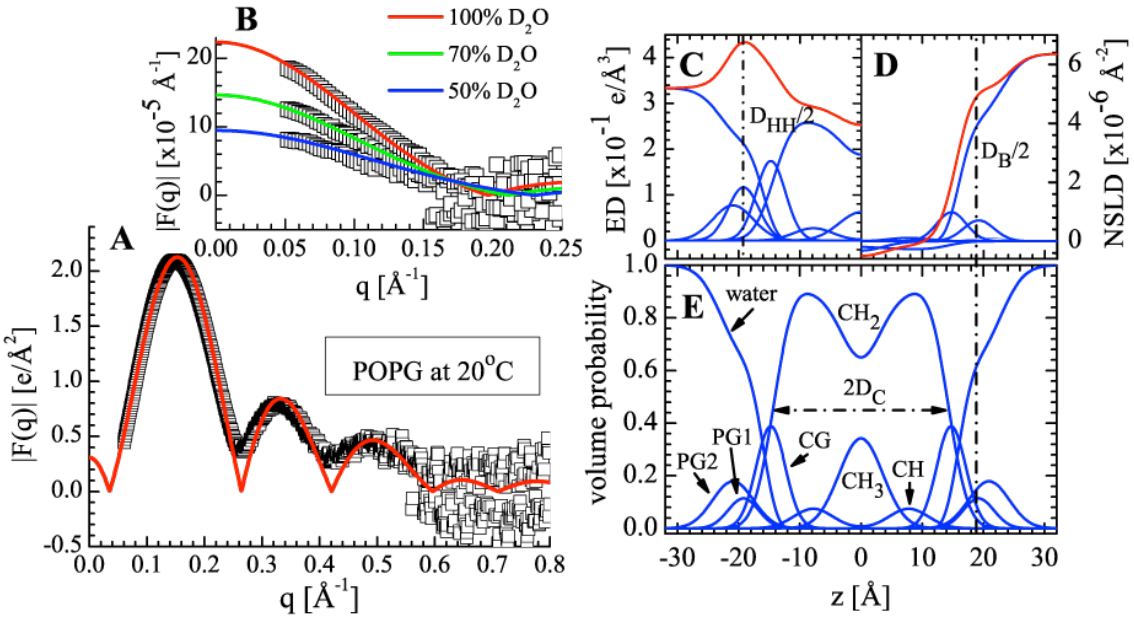

Fig. S12. SDP model analysis of POPG at 20°C.

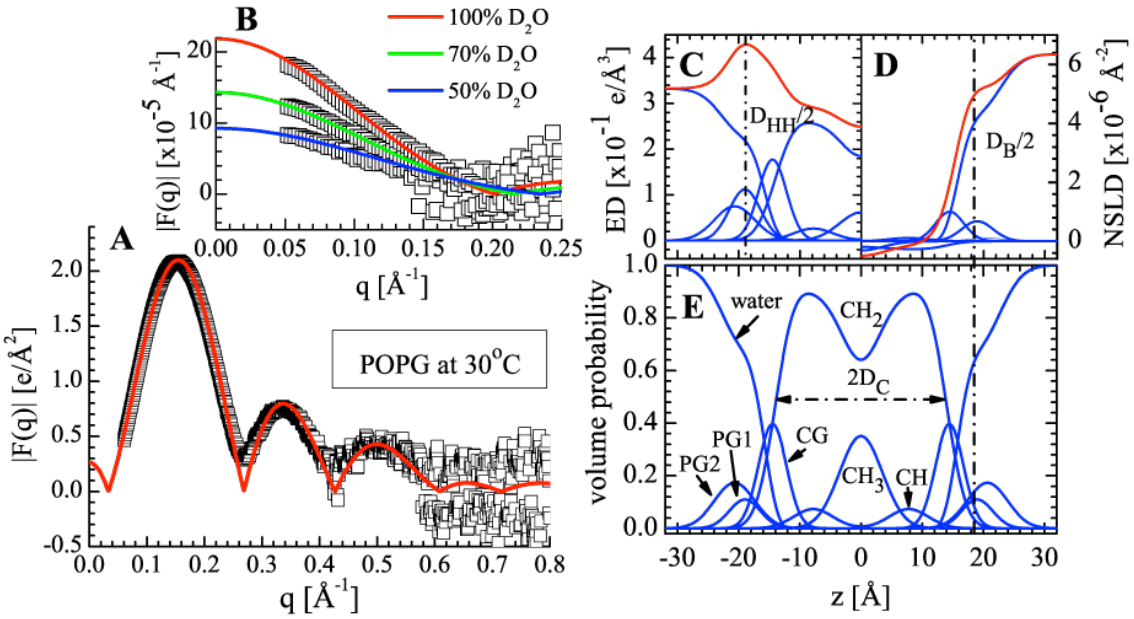

Fig. S13. SDP model analysis of POPG at 30°C.

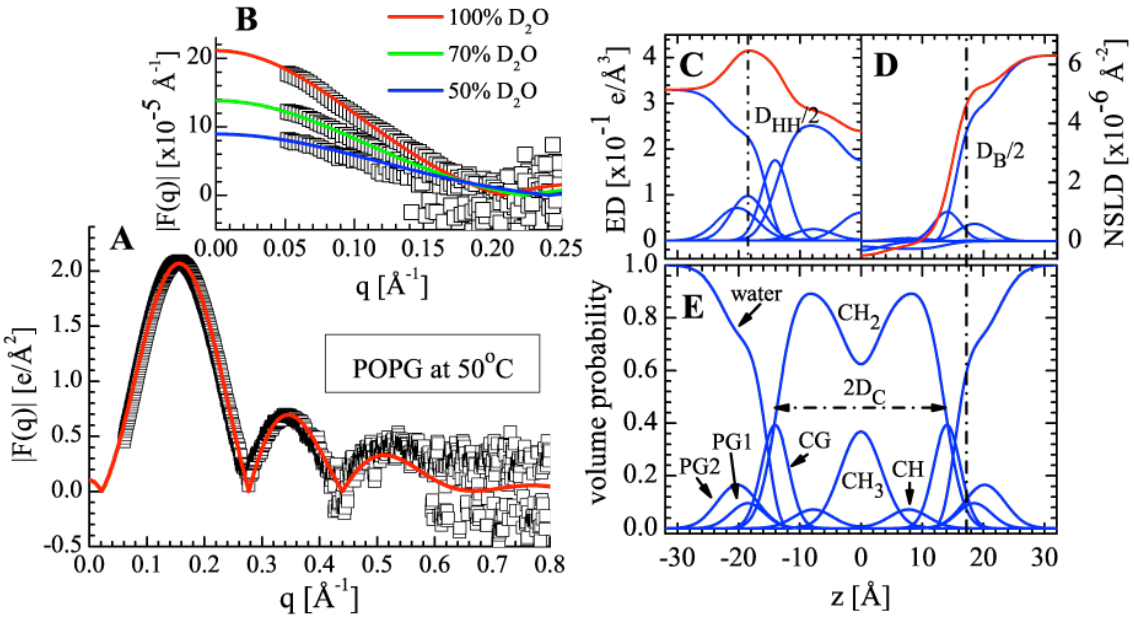

Fig. S14. SDP model analysis of POPG at 50°C.

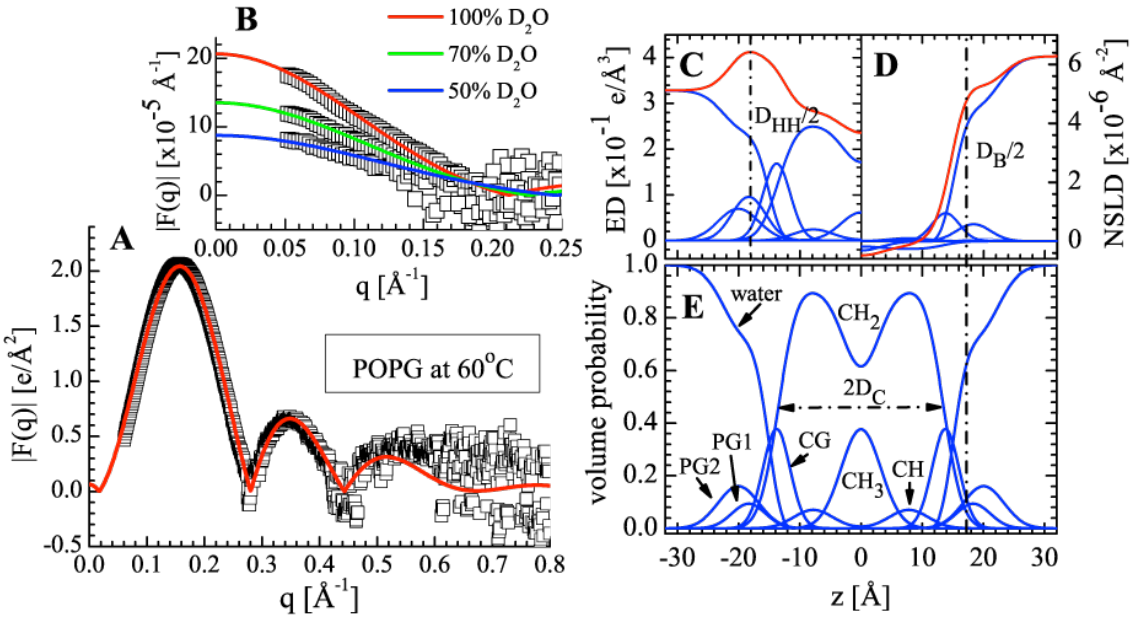

Fig. S15. SDP model analysis of POPG at 60°C.

Table S4 Length (Å), area (Å^2), and volume (Å^3) parameters for SOPG bilayers (estimated uncertainty of ±2%).

Figure	S15	S16	S17	S18
Lipid	SOPG	SOPG	SOPG	SOPG
T	20^{o}C	30^{o}C	50^{o}C	60^{o}C
V_L	1265.5**	1272.8**	1288.6**	1297.1**
V_{HL}	291.0**	291.0**	291.0**	291.0**
R_{CG}	0.52*(0.52)	0.52*(0.52)	0.52*(0.52)	0.52*(0.52)
R_{PG1}	0.14*(0.16)	0.15*(0.16)	0.16*(0.16)	0.16*(0.16)
r	1.76*(1.86)	1.81*(1.86)	1.89*(1.86)	1.87*(1.86)
r_{12}	0.68*(0.71)	0.69*(0.71)	0.71*(0.71)	0.71*(0.71)
D_B	38.8	38.2	37.1	36.6
D_{HH}	39.4	39.0	38.2	37.8
2Dc	29.9	29.5	28.7	28.4
D_{H1}	4.8	4.8	4.7	4.7
A	65.2	66.7	69.4	70.9
z_{CG}	15.8	15.5	14.9	14.7
σ_{CG}	2.45	2.36	2.13	2.05
z_{PG1}	20.0	19.8	19.4	19.1
σ_{PG1}	2.47	2.60	2.63	2.78
z_{PG2}	21.9	21.5	20.9	20.7
σ_{PG2}	3.30**	3.30**	3.30**	3.30**
z_{CH}	7.8**	7.8**	7.8**	7.8**
σ_{CH}	3.20**	3.20**	3.20**	3.20**
σ_{HC}	2.53*(2.44)	2.49*(2.44)	2.47*(2.44)	2.46*(2.44)
σ_{CH3}	3.60	3.53	3.30	3.00

**fixed parameters.

*soft-constrained parameters with target values shown in parentheses.

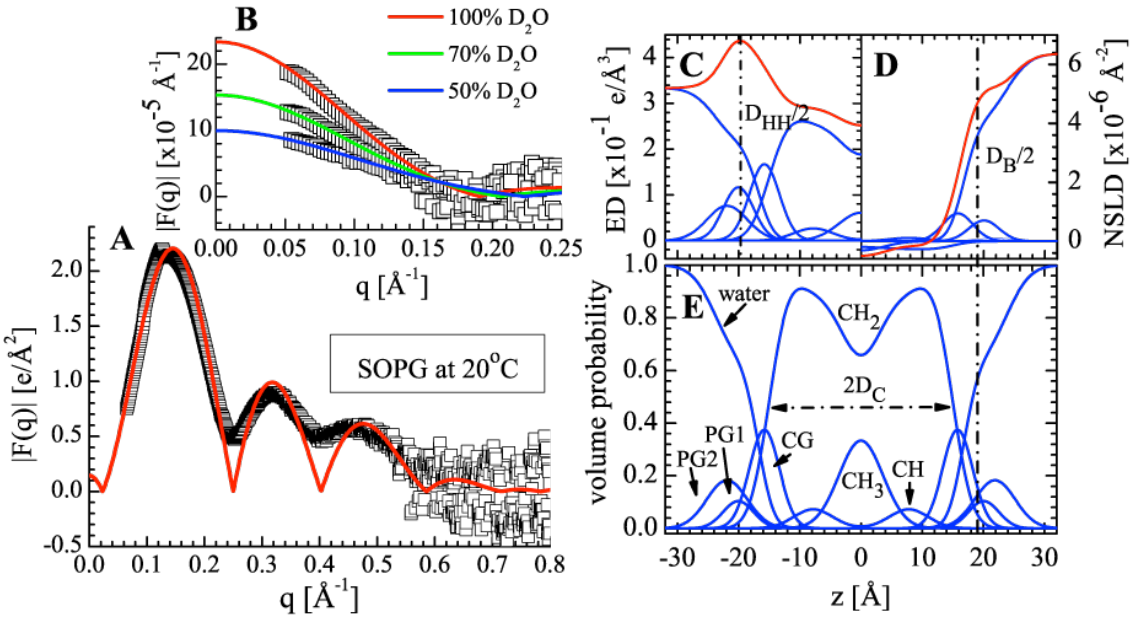

Fig. S16. SDP model analysis of SOPG at 20°C. As discussed in the main text, the small peak near 0.1Å^{-1} in the X-ray form factor is due to contamination from pauci-lamellar vesicles (PLVs). Much larger error uncertainties were thus assigned to data points near this peak in order to downplay any effects associated with the presence of PLVs.

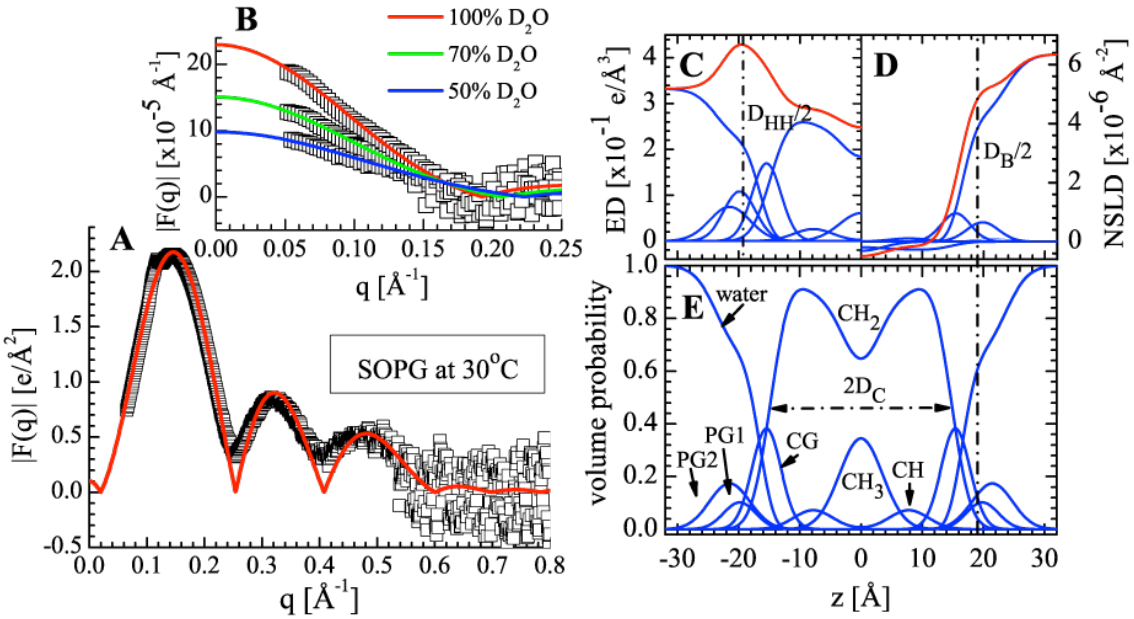

Fig. S17. SDP model analysis of SOPG at 30°C. The same PLV effect is seen as in Fig. S15.

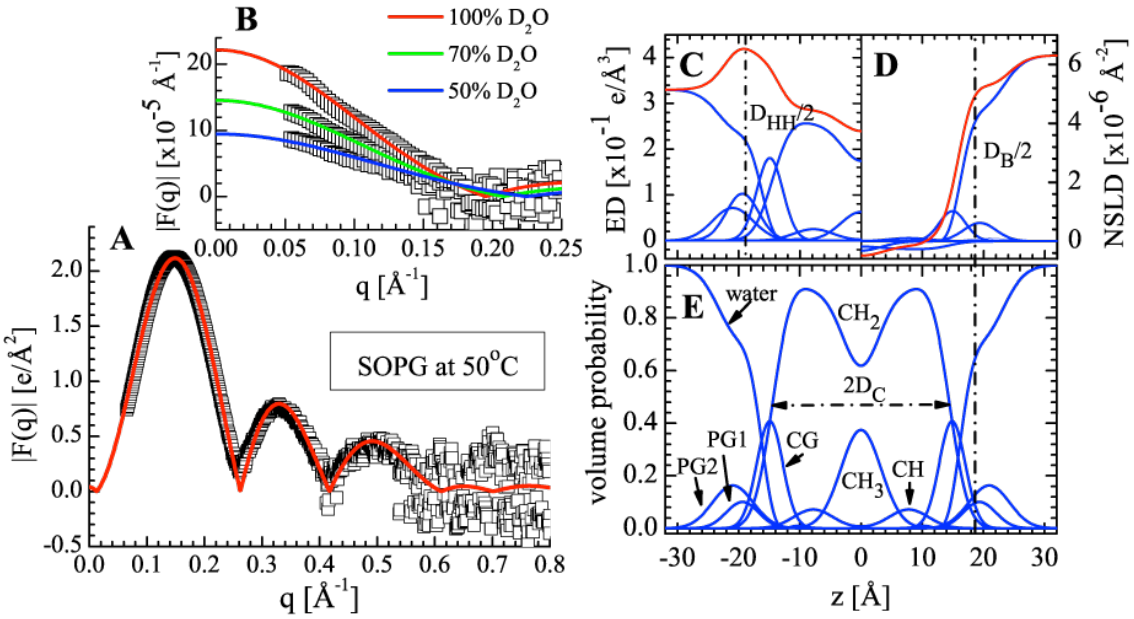

Fig. S18. SDP model analysis of SOPG at 50°C.

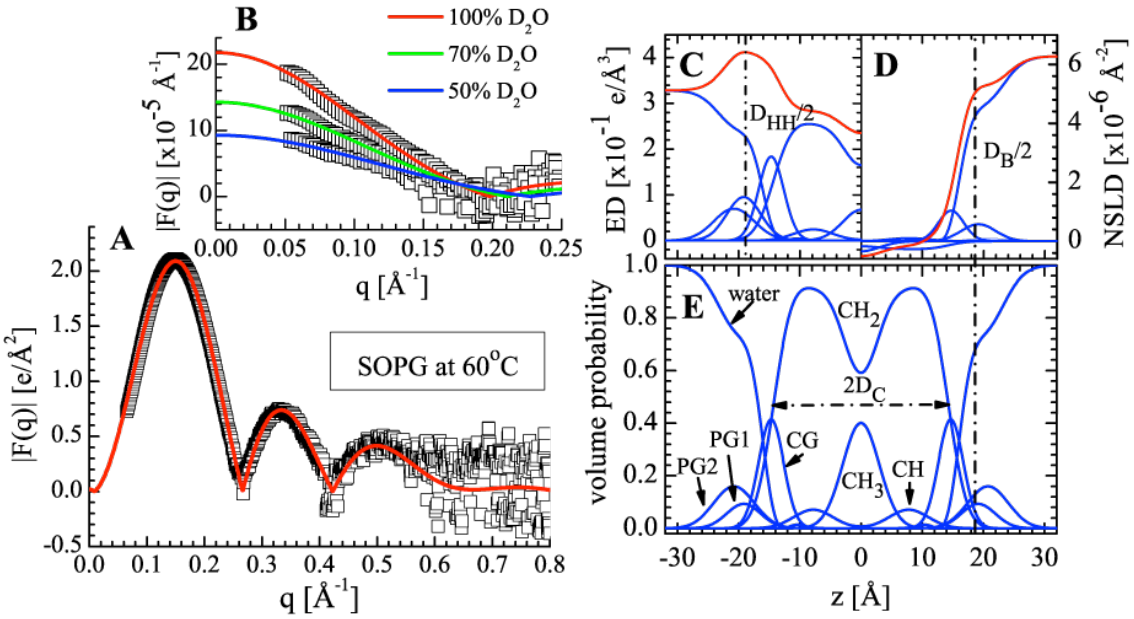

Fig. S19. SDP model analysis of SOPG at 60°C.

Table S5 Length (Å), area (Å^2), and volume (Å^3) parameters for DOPG bilayers (estimated uncertainty of ±2%).

Figure	S15	S16	S17	S18
Lipid	DOPG	DOPG	DOPG	DOPG
Temp	20°C	30°C	50°C	60°C
V_L	1257.5**	1265.0**	1281.0**	1288.2**
V_{HL}	291.0**	291.0**	291.0**	291.0**
R_{CG}	0.50*(0.52)	0.51*(0.52)	0.51*(0.52)	0.50*(0.52)
R_{PG1}	0.16*(0.16)	0.16*(0.16)	0.16*(0.16)	0.16*(0.16)
r	1.76*(1.86)	1.82*(1.86)	1.84*(1.86)	1.84*(1.86)
r_{12}	0.76*(0.71)	0.71*(0.71)	0.71*(0.71)	0.70*(0.71)
D_B	36.3	35.7	35.1	35.0
D_{HH}	36.0	36.2	35.6	35.6
2Dc	27.9	27.5	27.2	27.1
D_{H1}	4.1	4.3	4.2	4.2
A	69.4	70.8	72.9	73.6
z_{CG}	14.5	14.3	14.1	14.0
σ_{CG}	2.28	2.29	2.27	2.42
z_{PG1}	18.8	18.7	18.5	18.5
σ_{PG1}	2.74	2.73	2.76	2.75
z_{PG2}	18.8	18.6	18.5	18.5
σ_{PG2}	3.30**	3.30**	3.30**	3.30**
z_{CH}	7.8**	7.8**	7.8**	7.8**
σ_{CH}	3.20**	3.20**	3.20**	3.20**
σ_{HC}	2.56*(2.44)	2.59*(2.44)	2.56*(2.44)	2.63*(2.44)
σ_{CH3}	3.81	4.08	3.50	3.14

**fixed parameters.

*soft-constrained parameters with target values shown in parentheses.

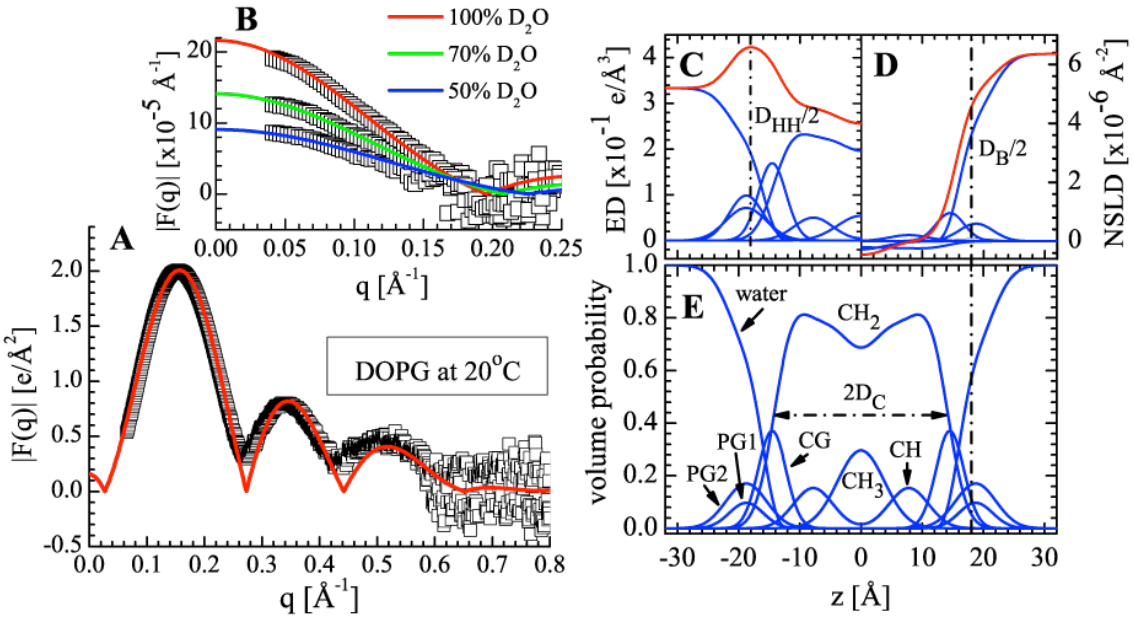

Fig. S20. SDP model analysis of DOPG at 20°C.

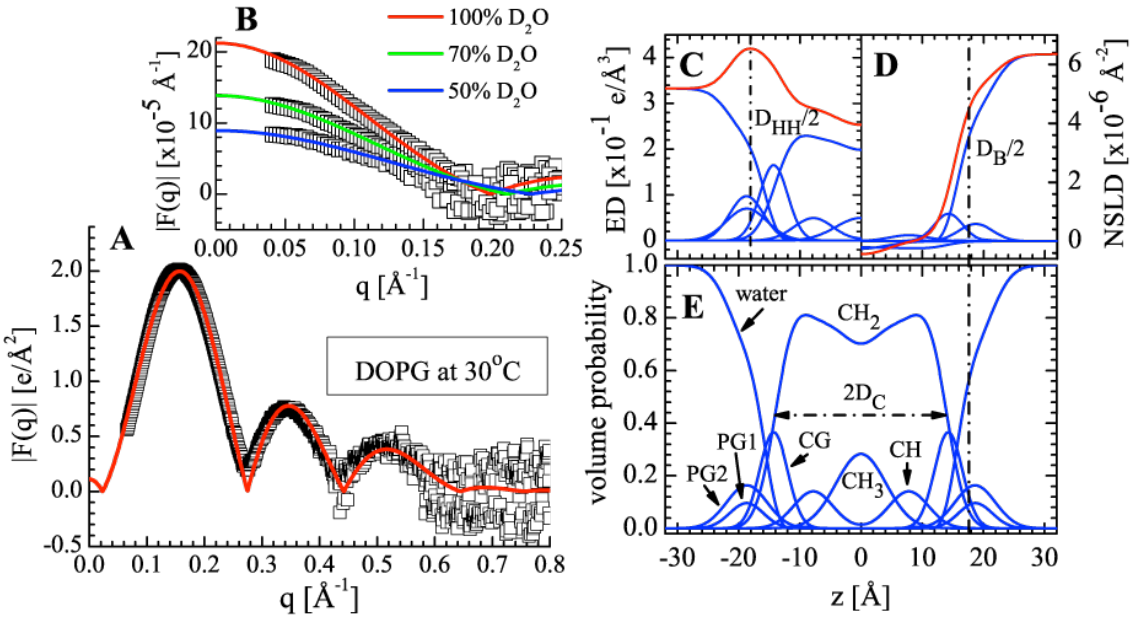

Fig. S21. SDP model analysis of DOPG at 30°C.

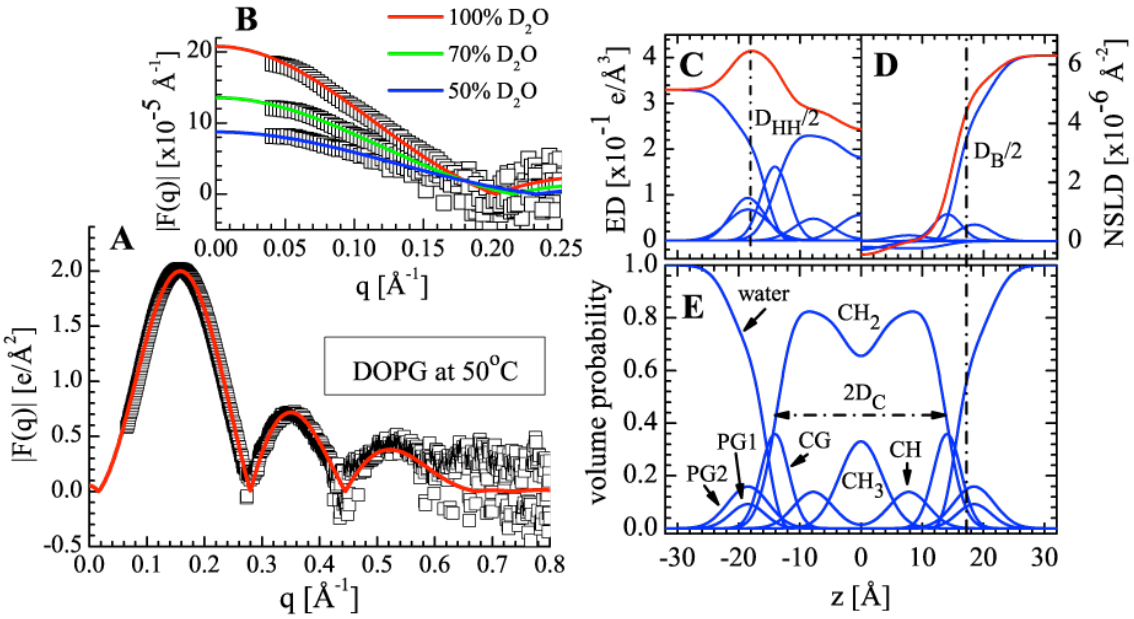

Fig. S22. SDP model analysis of DOPG at 50°C.

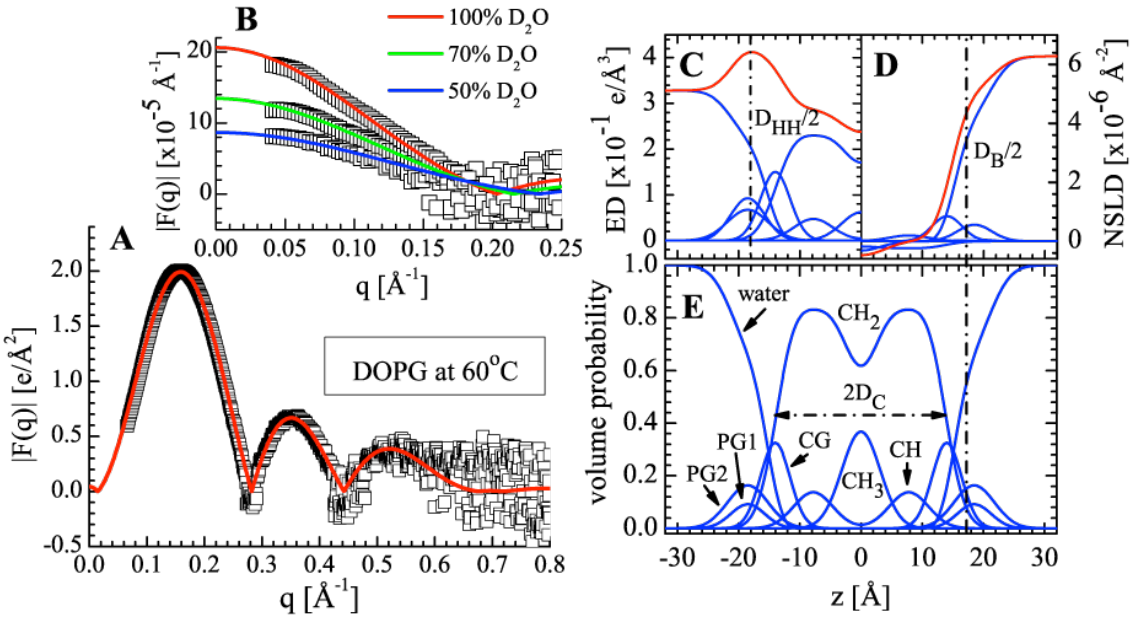

Fig. S23. SDP model analysis of DOPG at 60°C.

References

[S1] N. Kučerka, B.W. Holland, C.G. Gray, B. Tomberli, J. Katsaras, Scattering density profile model of POPG bilayers as determined by molecular dynamics simulations and small-angle neutron and X-ray scattering experiments, Journal of Physical Chemistry B, 116 (2012) 232-239.

[S2] N. Kučerka, J.F. Nagle, J.N. Sachs, S.E. Feller, J. Pencer, A. Jackson, J. Katsaras, Lipid bilayer structure determined by the simultaneous analysis of neutron and X-ray scattering data, Biophysical Journal, 95 (2008) 2356-2367.

[S3] N. Kučerka, J. Katsaras, J.F. Nagle, Comparing membrane simulations to scattering experiments: introducing the SIMtoEXP software, Journal of Membrane Biology, 235 (2010) 43-50.